JMEPEG (2004) 13:257-264
DOI: 10.1361/10599490419144

1059-9495/$19.00

An Experimental Evaluation of the Effects of Ripple Current Generated by the Power Conditioning Stage on a Proton Exchange Membrane Fuel Cell Stack

Woojin Choi, Gyubum Joung, Prasad N. Enjeti, and Jo W. Howze

(Submitted 2 January 2004)

In this article, an impedance model of the proton exchange membrane fuel cell stack (PEMFCS) is proposed. The proposed study employs an equivalent circuit of the PEMFCS derived by the frequency response analysis technique. An equivalent circuit for the PEMFCS is developed to evaluate the effects of ripple currents generated by the power-conditioning unit. The calculated results are then verified by means of experiments using a commercially available PEMFCS. The relationship between ripple current and fuel cell performance, such as power loss and fuel consumption, is investigated. Experimental results show that the ripple current can contribute up to a 6% reduction in the available output power.

Keywords current ripple, frequency response analysis, fuel cell, impedance, modeling, power reduction, proton exchange membrane fuel cell

1. Introduction

In the 21st century, fuel cells appear to be poised to meet the power needs of a variety of applications. Fuel cells are electrochemical devices that convert chemical energy to electricity and thermal energy. Fuel cell systems are available to meet the needs of applications ranging from portable electronics to utility power plants. In addition to the fuel cell stack itself, a fuel cell system includes a fuel processor and subsystems to manage air, water, thermal energy, and power. The overall system is efficient at full load and part load, is scaleable to a wide range of sizes, is environmentally friendly, and potentially is competitive with conventional technology in first costs. Promising applications for fuel cells include portable power, transportation, building cogeneration, and distributed power for utilities. For portable power, a fuel cell coupled with a fuel container can offer a higher energy storage density and more convenience than conventional battery systems. In transportation applications, fuel cells offer higher efficiency and better part-load performance than conventional engines. In stationary power applications, low emissions permit fuel cells to be located in high-power density areas where they can supplement the existing utility grid. Furthermore, fuel cell systems can be directly connected to a building to provide both power and heat with cogeneration efficiencies as high as 80%.

Various attempts are being made to model proton exchange membrane fuel cell stack (PEMFCS). Almost all recent endeavors of modeling[1-4] have neglected the effects of inverter load due to reasons of simplicity. Several modeling methods have been suggested in the literature.[1-5] However, these modeling methods require fuel cell design parameters that are not easily obtainable. Furthermore, most of the models include complex chemical equations, which are not easy to solve and are not suitable for observing the electrical phenomena occurring when the fuel cell interacts with its power-conditioning unit. Therefore, a simple electrical model of the fuel cell stack must be developed that can be used to electrically explain the nature of the fuel cell when it works along with its power conditioner. In this study, these crucial effects of inverter loads are considered, thus providing a vivid and brighter picture of the dynamics of the PEMFCS.

Since the fuel cell produces direct current (DC) electricity, a power-conditioning stage is essential to produce commercial alternating current (AC) power (120 V, 60 Hz). A typical fuel cell power-conditioning unit employs switch-mode DC-DC and DC-AC converters with state-of-the-art power semiconductor devices (Fig. 1). An important variable in the design of the power conditioner for a fuel cell is the amount of ripple current that the fuel cell can tolerate. Both the magnitude and frequency of the ripple current are important. For fuel cells powering single-phase loads (60 Hz), the ripple current is twice the output frequency (i.e., 120 Hz). The effect of the ripple current on the performance of a fuel cell stack has not been investigated thoroughly and, so far, remains uncertain.[5]

In this article, an experimental evaluation of the effects of ripple current generated by the power-conditioning stage on a

This paper was presented at the Fuel Cells: Materials, Processing, and Manufacturing Technologies Symposium sponsored by the Energy/Utilities Industrial Sector & Ground Transportation Industrial Sector and the Specialty Materials Critical Technologies Sector at the ASM International Materials Solutions Conference, October 13-15, 2003, in Pittsburgh, PA. The symposium was organized by P. Singh, Pacific Northwest National Laboratory, S.C. Deevi, Philip Morris USA, T. Armstrong, Oak Ridge National Laboratory, and T. Dubois, U.S. Army CECOM.

W. Choi, P.N. Enjeti, and J.W. Howze, Power Electronics & Fuel Cell Power-Conditioning Laboratory, Department of Electrical Engineering, Texas A&M University, College Station, TX 77843; and **G. Joung,** Power Electronics Research Laboratory, Department of Information and Communication Engineering, Woosuk University, Woosuk University, Iksan, 565-701 Korea. Contact e-mail: enjeti@tamu.edu.

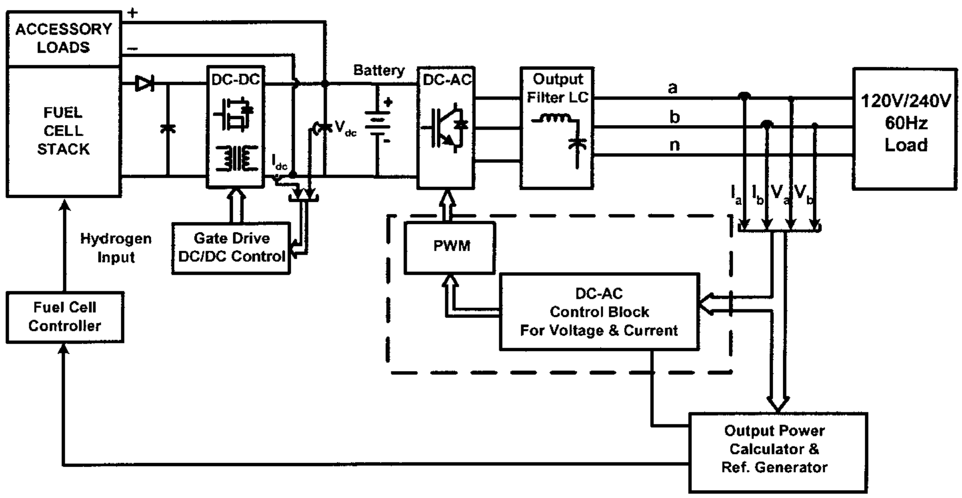

Fig. 1 Block diagram of a fuel cell power generation unit for supplying 120 V/240 V, 60 Hz load

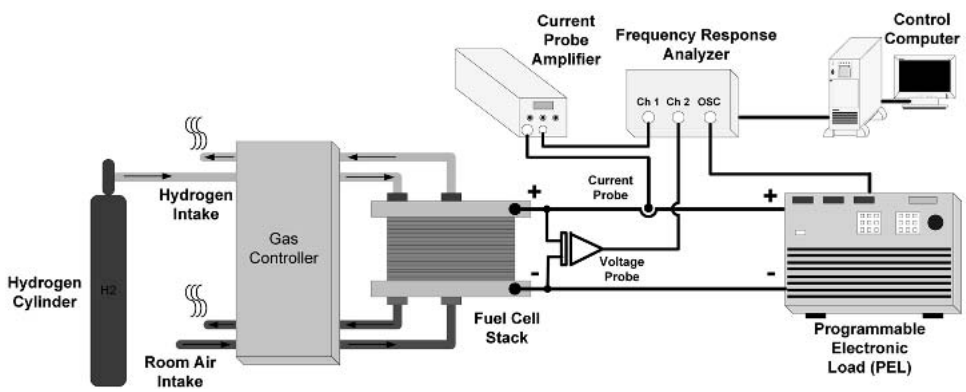

Fig. 2 FRA technique: experimental setup for the PEMFCS

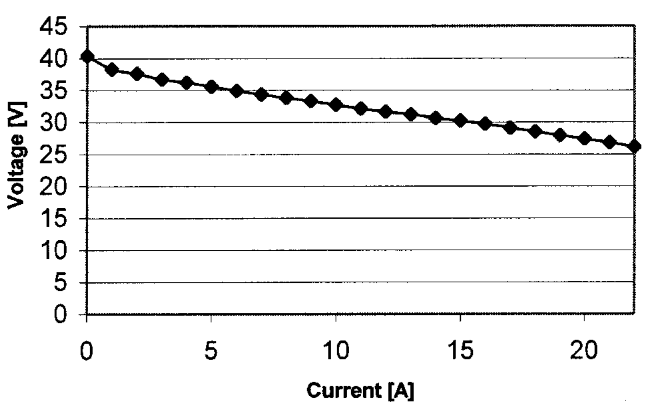

Fig. 3 Polarization curve (V-I) of the PEMFCS

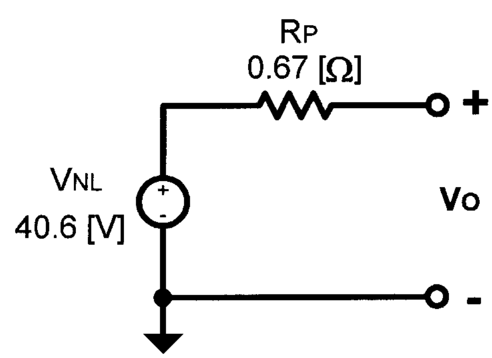

Fig. 4 DC equivalent circuit of the PEMFCS at a certain operating point

commercially available PEMFCS is presented. The proposed study employs an equivalent circuit of the PEMFCS derived by the frequency response analysis (FRA) technique. An equivalent circuit for the PEMFCS developed for evaluating the effects of ripple current generated by the power-conditioning unit. The calculated results are then verified by means of experiments on a commercially available 500 W PEMFCS (Avistalabs, Spokane, WA). The relationship between ripple current and fuel cell stack performance such as power loss and fuel consumption is investigated.

Experimental results have indicated that ripple current can contribute up to a 6% reduction in the available output power. This article provides a detailed evaluation of these aspects and includes a discussion of the frequency dependency of the fuel cell equivalent circuit parameters. The results obtained are presented in per-unit form to facilitate easy comparison.

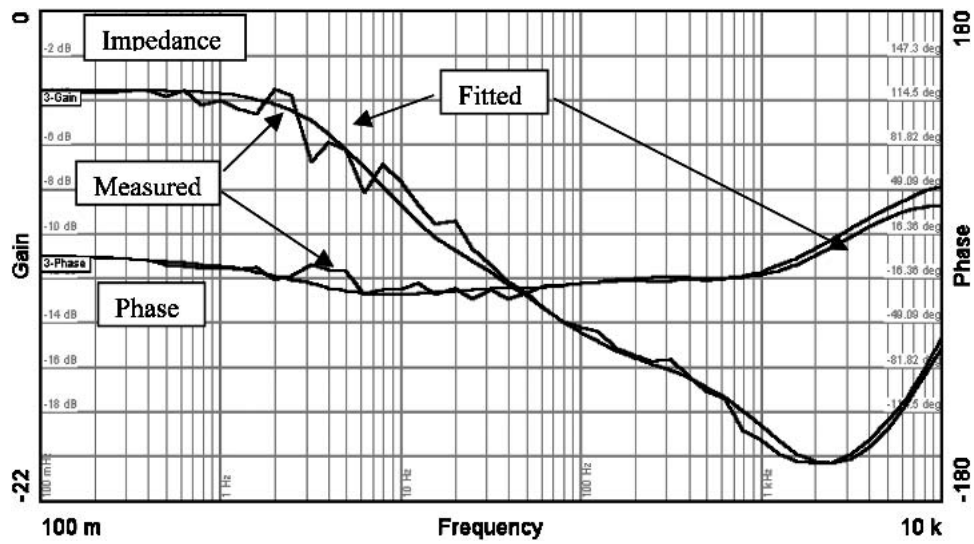

Fig. 5 Measured impedance spectrum of the PEMFCS and its curve-fitting results

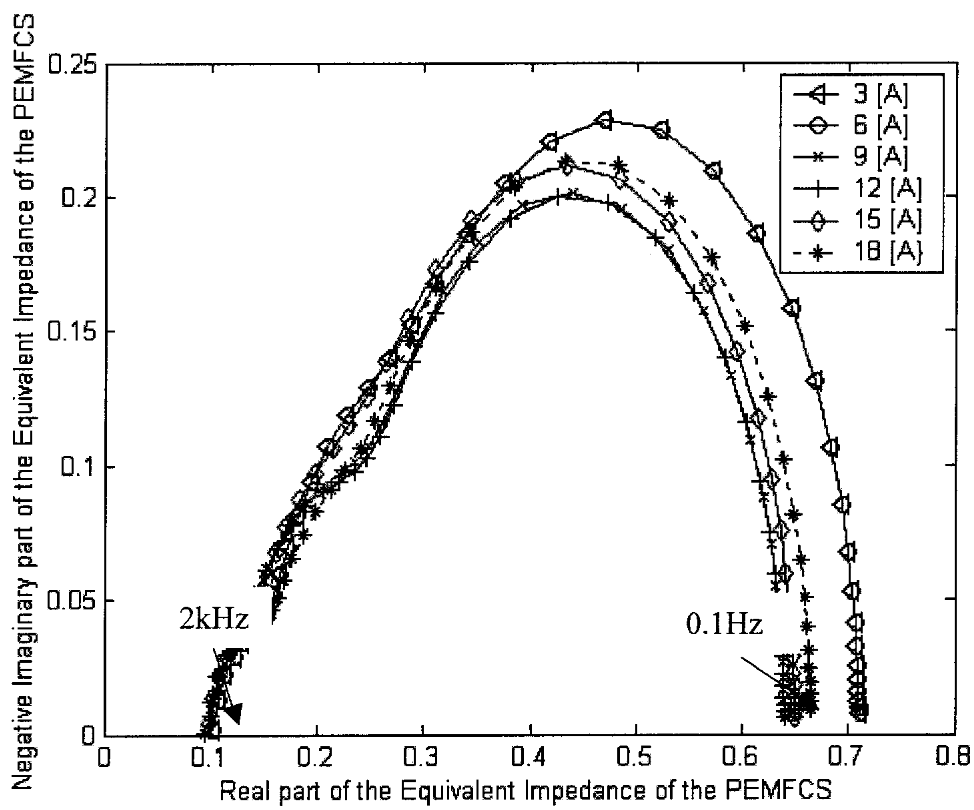

Fig. 6 Nyquist impedance plot of the PEMFCS

2. Modeling of the PEMFCS Using the FRA Technique

Figure 2 shows the experimental setup to evaluate the performance of the PEMFCS under a test load. The setup consists of a 500 W PEMFCS (Table 1), a programmable electronic load (Model 63201, Chroma, Irvine, CA), a frequency response analyzer (Model 260, Venable, Austin, TX), a current amplifier A6302 current probe (Model AM 503B, Tektronix, Inc., Baeverton, OH), a differential voltage probe (Model P5205, Tektronics, Baeverton, OR), and a computer with the Venable software. The test setup is used to perform both DC and AC tests described in the next sections.

Table 1. Specifications of 500 W PEMFCS (SR-12, Avistalabs)

Specification	Values
Power Output (Cont.)	500 W
Output voltage	25-39 V DC
Fuel source	Hydrogen
Fuel consumption	7.0 L/min at 500 W (<1.0 L/min at no load)
System start time	7 min at room temperature
Turndown ratio	500 W to no load, infinity
Operating temperature	5-35 °C
Dimension	22.3 × 24.2 × 13.6″
Weight	44 kg per cartridge

2.1 DC Equivalent Circuit

In this test, the fuel cell is supplied with hydrogen, and the electrical load (DC) is varied from zero to full load (rated). The fuel cell terminal voltage variation is plotted for various output current settings (Fig. 3). This V-I curve is termed the fuel cell polarization curve. The V-I curve is somewhat nonlinear for lower values of current but exhibits a near linear behavior for a load current of >25%. If the initial non-linearity is neglected, a simplified electrical equivalent circuit for the fuel cell can be obtained by calculating the slope of the V-I curve (Fig. 3). Figure 4 shows the equivalent circuit with a resistance of 0.67 Ω in series with 40.6 V. The resistance is mainly due to the electrolyte and cell interconnects.

To facilitate the comparison between different ratings or kinds of fuel cell stacks, a per-unit system was adopted. For example, the PEMFCS modeled above is per-unitized from the polarization curve (Fig. 3) as follows:

V_{base} = 28.9 V: Voltage at the rated load
I_{base} = 17.3 A: Rated current (rms)
P_{base} = 500 W: Rated power
$R_{base} = V_{base}/I_{base} = 1.67\ \Omega$: Base impedance (Eq 1)

The resistance R_P shown in the fuel cell equivalent circuit (Fig. 4) can be represented in per-unit terms as

$$R_{P,per\text{-}unit} = \frac{R_P}{R_{base}} = \frac{0.67}{1.67} = 0.40 \text{ or } 40\% \quad \text{(Eq 2)}$$

Since the fuel cell V-I curve shows a wide variation in output voltage (V_o) from no load to full load, the voltage regulation factor (VRF) is defined as

$$\text{VRF} = \frac{V_{o,no\text{-}load} - V_{o,full\text{-}load}}{V_{o,full\text{-}load}} \quad \text{(Eq 3)}$$

It can be shown from Eq 1 that,

$$\text{VRF} = R_{P,Per\text{-}unit} = \frac{40.6 - 28.9}{28.9} \cdot 100 = 40\% \quad \text{(Eq 4)}$$

If another manufacturer's fuel cell $R_{P,Per\text{-}unit}$ is higher than the above value, then the above fuel cell is considered to be better from the electrical performance point of view.

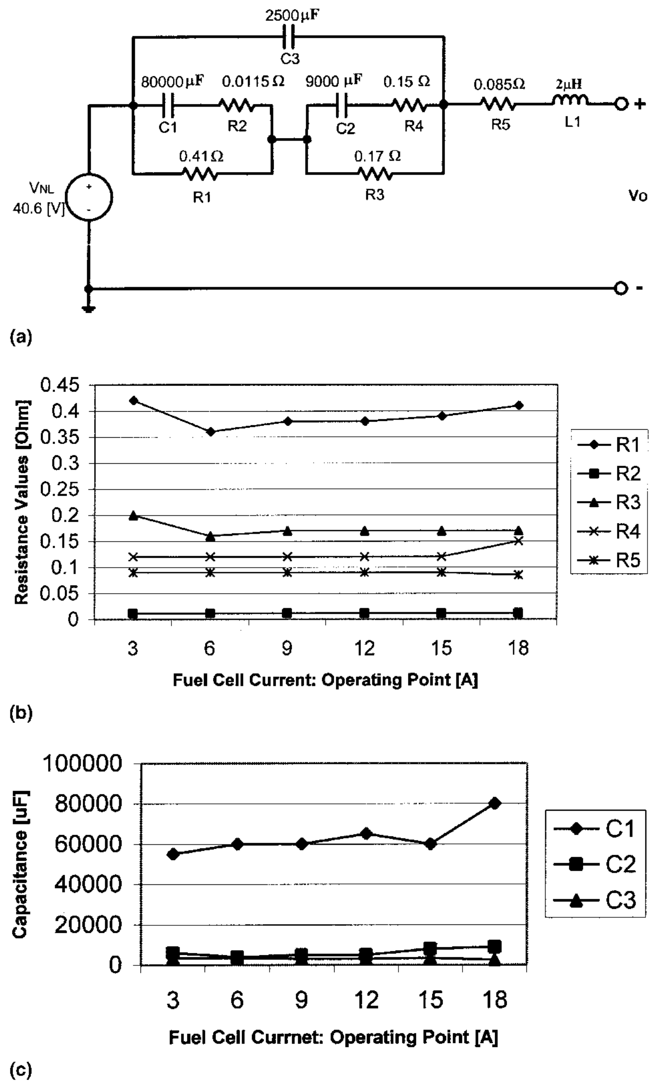

Fig. 7 **(a)** Equivalent circuit of the PEMFCS at the operating point of 18 [A], **(b)** variation of resistance values in the equivalent circuit shown in (a), and **(c)** variation of capacitance values in the equivalent circuit shown in (a).

2.2 AC Equivalent Circuit

The objective of this test was to obtain the AC impedance of the fuel cell stack from 0-10 kHz. In the test (Fig. 2), the fuel cell is operated at a certain operating point on the V-I curve. Now a small magnitude of sinusoidal AC current is superimposed on the DC current. The corresponding voltage (AC) at the fuel cell terminals is recorded. From these data, the AC impedance of the fuel cell is computed. The above test was repeated from 0-10 kHz, and the frequency response of fuel cell internal impedance was computed. Figure 5 shows the magnitude and phase plot of the fuel cell internal impedance from 0-10 kHz (for a DC current of 18 A, perturbed by a sinusoidal AC current of 1 A in magnitude). The above impedance test was repeated at different operating points on the fuel cell V-I curve (3-18 A). Figure 6 shows the Nyquist impedance plot of the computed impedance variation.

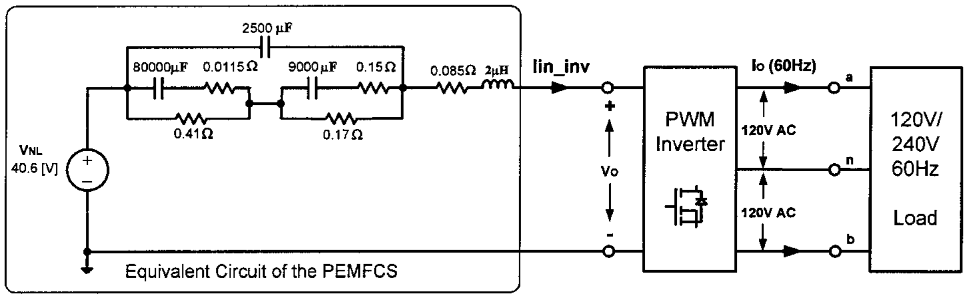

Fig. 8 Interconnection of the fuel cell equivalent circuit with the power-conditioning unit to facilitate the evaluation of the effect of ripple current

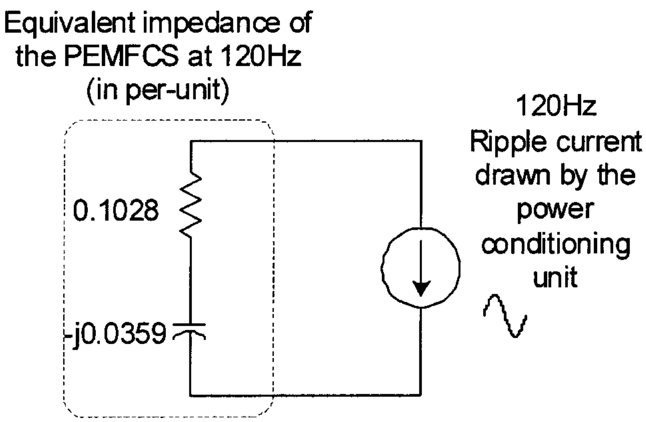

Fig. 9 AC equivalent circuit of the PEMFCS at 120 Hz

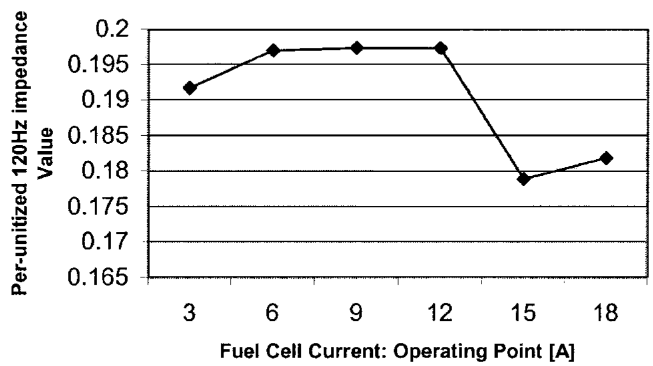

Fig. 10 Variation of 120 Hz impedance $|Z_{120Hz,per\text{-}unit}|$ for different DC current operating points

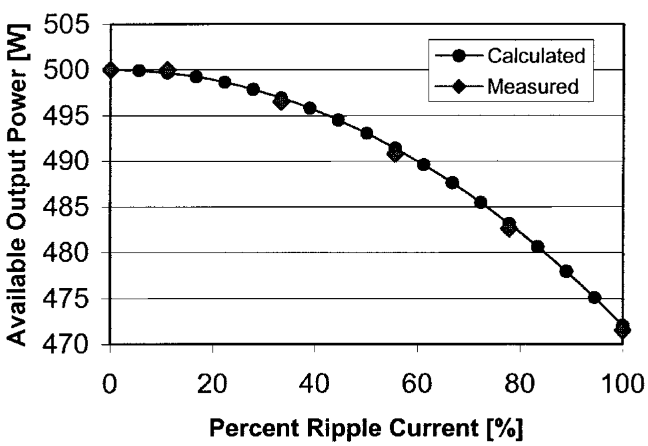

Fig. 11 Relationship between output power reduction and ripple current at the rated condition (17.3 A, 28.9 V, 500 W)

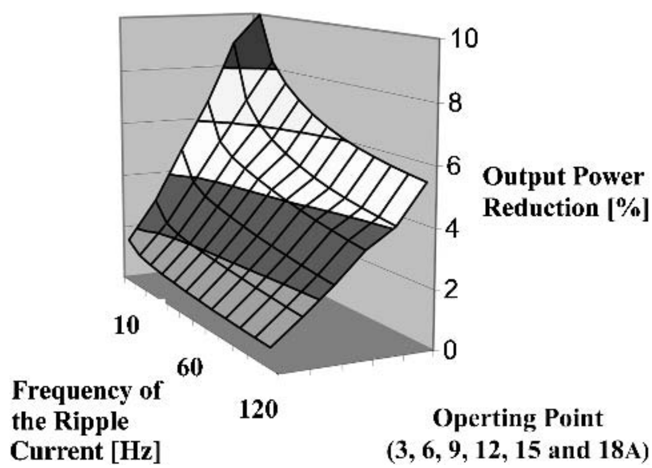

Fig. 12 Power reduction of the PEMFCS with a maximum ripple current at each operating point (3, 6, 9, 12, 15, and 18 A)

With the above-measured impedance data, an electrical equivalent circuit of the fuel cell internal impedance was obtained. Since one semicircle in the Nyquist impedance plot (Fig. 6) corresponds to a single time constant (R-C), closer observation of Fig. 6 shows the existence of three such time constants. Further, the diameter of each semicircle is a representative of the resistor value, while the vertex corresponds to the characteristic frequency. Using the above-described approach and the least square curve-fitting techniques, an electric equivalent circuit of the fuel cell was obtained from the measured data and is shown in Fig. 7(a). The equivalent circuit consists of R-C branches obtained from parameter extraction. The fitted curve (Fig. 5), which represents the frequency response (obtained from the equivalent circuit (Fig. 7a) shows the close agreement with the measured frequency data. It is clear from Fig. 7 that for DC conditions (zero frequency) the equivalent circuit parameters match the steady-state V-I data shown in Fig. 3 and 4. Fig. 7(b) and (c) show the variation of

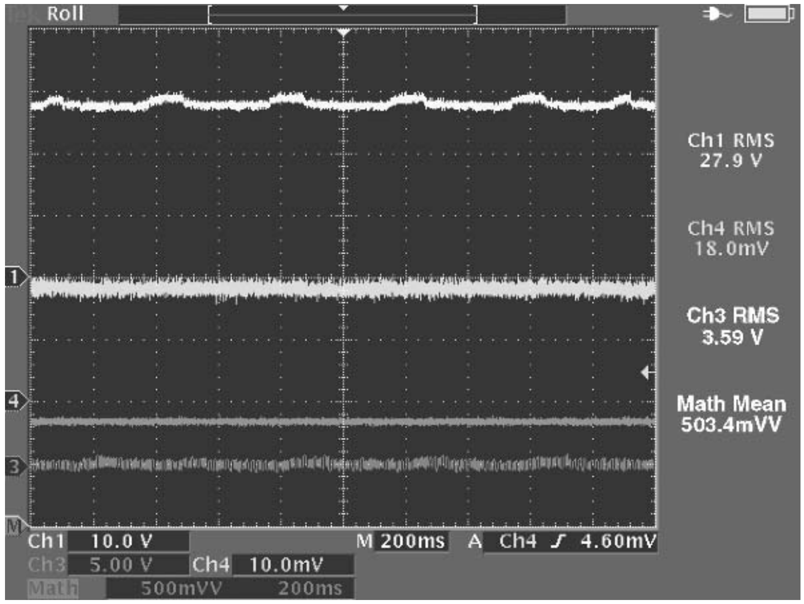

Fig. 13 PEMFCS loaded by a constant load (18 A). Channel-1, PEMFCS voltage (10 V/div); channel-4, PEMFCS current (10 A/div); channel-3, hydrogen flow rate (10 SLM/div); channel-M, PEMFCS output power (500 W/div), $P_o = 503.4$ W; div, division; SLM, standard liter per minute

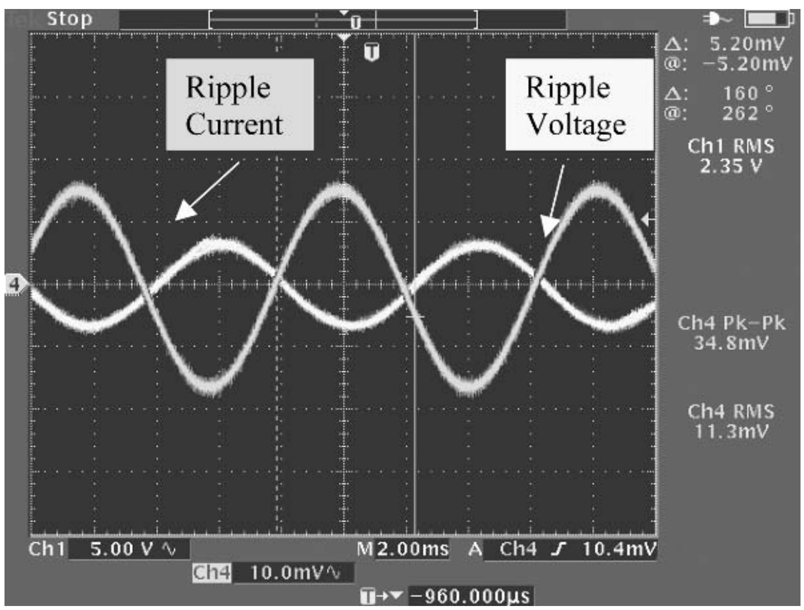

Fig. 14 Fuel cell terminal voltage and the ripple current for: 120 Hz ripple current (17.3 A, peak-to-peak value) at the DC operating point of 18 A, $P_o = 473.9$ W; hydrogen flow rate, 7.18 SLM/min; SLM, standard liter per minute

the equivalent circuit parameters for various DC operating points.

3. Evaluation of the Effect of Inverter Ripple Current

An important variable in the design of the power conditioner for fuel cell is the amount of ripple current the fuel cell can withstand. Since the reactant utilization is known to impact the mechanical nature of a fuel cell, it is suggested in Ref. 5 that the varying reactant conditions surrounding the cell (due to ripple current) govern, at least in part, the lifetime of the cells. Both the magnitude and frequency of the ripple current are important. For fuel cells powering single-phase loads (60 Hz), the ripple current of concern is twice the output frequency (i.e., 120 Hz).[6] A limit of 0.15 per unit (i.e., 15% of its rated current) from 10-100% load is specified.[7] Further, the magnitude of the low-frequency ripple current drawn from the fuel cell by the DC-DC converter is largely dependent on the volt-

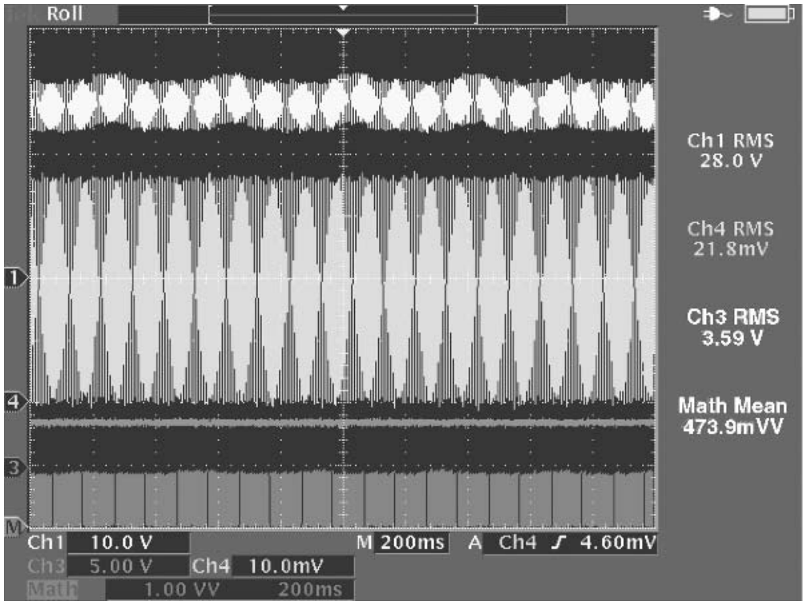

Fig. 15 PEMFCS loaded by a constant load (18 A) and a 120 Hz ripple (18 A peak-to-peak). Channel-1, PEMFCS voltage (10 V/div); channel-4, PEMFCS current (10 A/div); channel-3, hydrogen flow rate (10 SLM/div); channel-M, PEMFCS output power (1 kW/div); P_o = 473.9 W; div, division; SLM, standard liter per minute

age loop response characteristics. Also the DC-link capacitor size determines the 120 Hz voltage ripple on the DC-link, which in turn has an impact on the input current drawn from the fuel cell. It should be noted that switching frequency components in the DC-DC converter can be easily filtered via a small high-frequency capacitive filter.

This power-conditioning unit may be composed of any combination of switch-mode DC-DC converters, DC-AC inverters, filters, and isolation transformers, depending on the topology adopted.[6-10] Figure 8 shows the interconnection of the developed fuel cell equivalent circuit with the power-conditioning unit. Figure 9 shows the AC equivalent circuit of the fuel cell at 120 Hz frequency. This figure is obtained by setting f = 120 Hz in Fig. 7(a). Figure 10 shows the 120 Hz impedance variation for different DC current loading conditions of the fuel cell.

From Fig. 9, the impedance of the fuel cell stack at 120 Hz while supplying 18 A DC current is:

$$Z_{120\mathrm{H_z}} = 0.1717 - j0.06 = 0.1818 \angle -19.26° \quad \text{(Eq 5)}$$

From the per-unit quantities defined in Eq 1:

$$Z_{120\mathrm{Hz,per\text{-}unit}} = \frac{Z_{120\mathrm{Hz}}}{Z_{\mathrm{base}}} = R_{120\mathrm{Hz,per\text{-}unit}} - jX_{120\mathrm{Hz,per\text{-}unit}}$$

$$= 0.1028 - j0.0359 = 0.1089 \angle -19.26° \quad \text{(Eq 6)}$$

From the per-unit representation of fuel cell AC impedance in Eq 6, it can be shown that the introduction of ripple current by the power-conditioning unit contributes to a reduction in the available output power or causes power loss in the fuel cell stack. The reduction in fuel cell output power due to ripple current can be computed as

$$P_{\mathrm{Loss,per\text{-}unit}} = I^2_{\mathrm{Ripple,per\text{-}unit}} \cdot R_{120\mathrm{Hz,per\text{-}unit}}\ \mathrm{(W)} \quad \text{(Eq 7)}$$

Therefore, for $I_{\mathrm{Ripple,per\text{-}unit}} = 0.5$ (i.e., 50%), from Eq 6 and 7 we have

$$P_{\mathrm{Loss,per\text{-}unit}} = 0.0257$$

which corresponds to a 2.57% reduction in the output power.

In addition to power reduction, the ripple current (120 Hz) also contributes to AC voltage ripple (120 Hz) at the fuel cell output terminals. The magnitude of the AC ripple voltage also can be computed from Fig. 9 as

$$V_{\mathrm{Ripple,per\text{-}unit}} = I_{\mathrm{Ripple,per\text{-}unit}} \cdot Z_{120\mathrm{Hz,per\text{-}unit}} \quad \text{(Eq 8)}$$

Therefore, for $I_{\mathrm{Ripple,per\text{-}unit}} = 0.5$ (i.e., 50%), from Eq 6 and 8, $V_{\mathrm{Ripple,per\text{-}unit}} = 0.0544$, which corresponds to 5.44%.

4. Experimental Results and Discussion

Several experiments were conducted on the PEMFCS setup (Fig. 2). Figure 11 shows the variation of fuel cell available power as a function of the ripple current predicted by Eq 7. It is noted that under the extreme case of 100% ripple (120 Hz), the available power is reduced by 6%. Figure 12 shows the variation of available power as a function of ripple current frequency (note that for this test the ripple current magnitude is adjusted to 100% at each DC operating point). It is clear from this figure that a maximum power reduction of 10% can occur at 10 Hz.

Figure 13 shows the terminal voltage, current, and hydrogen flow rate when the fuel cell is supplying a DC load current of 18 A. Figures 14 and 15 show the fuel cell terminal voltage when supplying a ripple current of 120 Hz. In addition, Fig. 15 confirms the power reduction due to the ripple current.

5. Conclusion

In this article, an impedance model of the PEMFCS has been experimentally developed. Experimental results show that the model explains the electrical characteristics of the fuel cell when connected to a power-conditioning unit. The relationships among ripple current, internal loss, and fuel consumption have been analyzed within the constraints of the model. It has been shown experimentally that the ripple current can contribute to a reduction in the fuel cell available output power, cause internal losses, and increase distortion of its terminal voltage. Limiting the low-frequency (120 Hz) fuel cell ripple current to 15-20% has been shown to result in less than 1% losses and, therefore, may be acceptable.

References

1. G. Maggio, V. Recupero, and L. Pino: "Modeling Polymer Electrolyte Fuel Cells: An Innovative Approach," *J. Power Source,* 2001, *101,* pp. 257-86.
2. J.C. Amphlett, R.F. Mann, B.A. Peppley, P.R. Roberge, and A. Rodrigues: "A Model Predicting Transient Responses of Proton Exchange Membrane Fuel Cells," *J. Power Source,* 1996, *61,* pp. 183-88.
3. K.Y. Lukas and H.G. Lee: "An Explicit Dynamic Model for Direct Reforming Carbonate Fuel Cell Stack," *IEEE Trans. Energy Conv.,* 2001, *16*(3), pp. 289-95.
4. J.M. Correa, F.A. Farret, and L.N. Canha: "An Analysis of the Dynamic Performance of Proton Exchange Membrane Fuel Cells Using an Electrochemical Model," *Proc. IECON'01,* November 29-December 2, 2001, Denver, CO, pp. 141-46.
5. R.S. Gemmen: "Analysis for the Effect of the Ripple Current On Fuel Cell Operating Condition," *ASME 2001 IMECE,* November 11-16, 2001, New York, NY.
6. P. Enjeti: "Power Conditioning Systems for Fuel Cell Systems," in *US Department of Energy Fuel Cell Handbook,* 6th ed. 2002.
7. Department of Energy. Future Energy Challenge: 2001 and 2003, Low Cost Fuel Cell Inverter Design Competition. Available at: http://www.energychallenge.org.
8. W. Choi, Jo. W. Howze, and P. Enjeti: "Fuel Cell Powered UPS System: Design Considerations," June 15-19, 2003, pp. 385-90.
9. P. Enjeti, M. Yeary, Jo. W. Howze, and C. Culp: *Texas A&M University Future Energy Challenge Team Final Report,* Texas A&M University, College Station, TX, 2001.
10. R. Gopinath, S. Kim, et al.: "Development of a Low Cost Fuel Cell Inverter System with DSP Control," *Proc. Power Electronics Specialists Conference 2002,* 23-27 June 2002, pp. 309-14.